Defence Science Journal, Vol. 56, No. 5, November 2006, pp. 701-713

Analysis of Titanium-matrix Orthotropic Cylindrical Shell Subjected to Thermomechanical Loading

M.C.S. Reddy and G. Rama Murty

Osmania University, Hyderabad–500 007

ABSTRACT

A titanium-matrix orthotropic cylindrical shell with the principal direction of orthotropy following a parallel constant angle helix, has been studied when it is subjected to uniform loading conditions of internal pressure, axial load and pure twisting moment. Nondimensional parameters pertaining to loading and deformations have been calculated and results plotted. The results obtained can be usefully applied in robotic actuators where lightweight considerations with high strength are of prime importance. The study is further extended to investigate the effect of temperature on the deformations. Through parametric studies, deformation patterns are calculated and plotted that are unique to orthotropy. In most of the cases, it is observed that deformation patterns are same, but deformation is increasing with temperatures.

Keywords: Titanium-matrix composites, orthotropic cylindrical shells, unconstrained effects, thermomechanical loading, deformation

NOMENCLATURE

θ_o	Fibre orientation angle
R	Mean radius of the shell
S_{ij}	Transformed compliance coefficients
Q_{ij}	Components of the lamina stiffness matrix
Q_{ij}	Components of the transformed lamina stiffness matrix
S_{ij}	Components of the transformed lamina compliance matrix
E_{ij}	Young's modulus
G_{ij}	Shear modulus
ν_{ij}	Poisson's ratio
ε_{ij}	Strains
σ_{ij}	Stresses
u_i	Displacements
p	Internal pressure
P	Uniform axial load
T	Uniform torque
φ_r	Angle of rotation
z	Axial coordinate
C_1-C_9	Nondimensional parameters
D_1-D_4	Nondimensional parameters
α_1	Coefficient of thermal expansions along to the fibre direction

Revised 11 January 2005

α_2 Coefficient of thermal expansions transverse to the fibre direction

1, 2, 3 Principal material coordinates

x, y, z Global coordinates

1. INTRODUCTION

Titanium-matrix composites with SCS6 fibres find wide applications in high-temperature environment. The aerospace, automotive and gas turbine industries share the never-ending quest for lighter and stronger materials suitable for use in increasingly demanding high-temperature environment. The development of composite materials, that have reduced weight and increased strength relative to the previously used materials, is critical to achieving the goal of higher operating temperatures, long life and reduced weight.

One such composite system is the titanium-based silicon carbide fibre-reinforced metal-matrix composite. Metal matrices have high strength, stiffness and ductility but at the expense of higher density. Silicon carbide fibres are used primarily in high-temperature metal-matrix composites because of their excellent oxidation resistance and high-temperature strength retention. Hence, it is interesting to study the behaviour of these composites when these are formed into a cylindrical shell and subjected to uniform loading conditions with temperature changes.

Many papers appeared in the analysis of orthotropic cylindrical shells. Wilkins and Love[1] analysed the combined compression and shear buckling behaviour of the laminated composite cylindrical shells characteristic of fuselage structures. Waltz and Vinson[2] presented the method of analysis for the determination of interlaminar stresses in laminated cylindrical shells of composite materials. Naschie[3] investigated the large deflection behaviour of composite material shells in determining the lower limit of the asymmetric buckling load.

Fujczak[4] studied the torsional fatigue behaviour of graphite-epoxy cylindrical shells. Bootan[5] investigated the buckling of imperfect composite material cylinders under the combined loading involving axial compression, external pressure and torsion. Montague[6] experimentally studied the behaviour of double-skinned composite, circular cylindrical shells subjected to external pressure. Ynceoglu and Updike[7] studied the stress concentrations in bonded, multilayer cylindrical shells.

Reissner and Tsai[8] reported the study of pure bending, stretching and torsion of anisotropic cylindrical shells. Wilson and Orgill[9] presented the linear analysis of uniformly stressed orthotropic cylindrical shells under uniform load conditions. The large coefficient of thermal expansion (CTE) mismatch between the matrix and fibre, leads to high tensile residual stresses at the fibre/matrix interface[10,11]. Wilson and Orgill studied the orthotropic cylindrical shells with approximation, whereas in the present study it has not been approximated.

In this paper, an attempt has been made to investigate the deformation of an orthotropic cylinder made out of titanium-matrix composite with SCS6 fibres when it is subjected to thermal loads[12] in addition to the following three types of mechanical loading:

(i) internal pressure (*p*),

(ii) longitudinal load (*P*) and

(iii) pure torque (*T*) causing rotation about the longitudinal axis.

The shear strain ($r_{\theta z}$), longitudinal strain ($\varepsilon_{zz)}$ and circumferential strain ($\varepsilon_{\theta\theta)}$ have been represented as nondimensional parameters expressed in terms of loading, fibre angle and material properties. The present study comprises the deformations caused when loads are applied separetely and also in combination.

The principal coordinate system and global coordinate system defined for the orthotropic cylinder are shown in Fig.1.

2. CONSTITUTIVE RELATIONSHIPS

The metal-matrix composites are considered with fibres oriented at angle θ_0 to the tangential direction of the tube in the plane r = Constant. The principal direction of orthotropy follows parallel

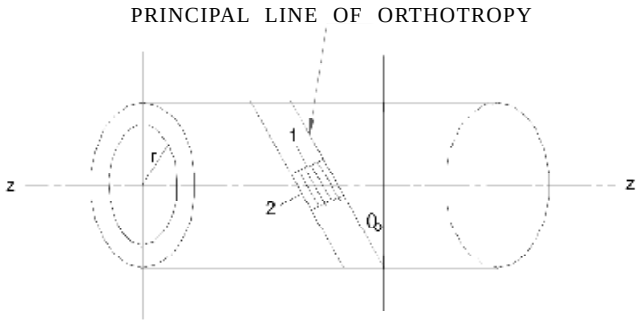

Figure 1. Coordinate system for the orthotropic cylinder.

constant helices. The constitutive relationship for an orthotropic elastic solid[13,14] relating the six components of strain to six components of stress expressed wrt to the principal material coordinates axes (1,2,3) are expressed as

$$\begin{bmatrix} e_{11} \\ e_{22} \\ e_{33} \\ ?_{12} \\ ?_{13} \\ ?_{23} \end{bmatrix} = \begin{bmatrix} 1/E_{11} & -?_{21}/E_{22} & -?_{31}/E_{33} & 0 & 0 & 0 \\ -?_{12}/E_{11} & 1/E_{22} & -?_{32}/E_{33} & 0 & 0 & 0 \\ -?_{13}/E_{11} & -?_{23}/E_{22} & 1/E_{33} & 0 & 0 & 0 \\ 0 & 0 & 0 & 1/G_{12} & 0 & 0 \\ 0 & 0 & 0 & 0 & 1/G_{13} & 0 \\ 0 & 0 & 0 & 0 & 0 & 1/G_{23} \end{bmatrix} \begin{bmatrix} s_{11} \\ s_{22} \\ s_{33} \\ s_{12} \\ s_{13} \\ s_{23} \end{bmatrix} \tag{1}$$

The constitutive relationship from the principal coordinates can be transformed into global coordinates (r,θ,z) and can be expressed as

$$\begin{bmatrix} \varepsilon_{\theta\theta} \\ \varepsilon_{zz} \\ \varepsilon_{rr} \\ \gamma_{rz} \\ \gamma_{r\theta} \\ \gamma_{\theta z} \end{bmatrix} = \begin{bmatrix} S_{11} & S_{12} & S_{13} & 0 & 0 & S_{16} \\ S_{21} & S_{22} & S_{23} & 0 & 0 & S_{26} \\ S_{31} & S_{32} & S_{33} & 0 & 0 & S_{36} \\ 0 & 0 & 0 & S_{44} & S_{45} & 0 \\ 0 & 0 & 0 & S_{54} & S_{55} & 0 \\ S_{61} & S_{62} & S_{63} & 0 & 0 & S_{66} \end{bmatrix} \begin{bmatrix} \sigma_{\theta\theta} \\ \sigma_{zz} \\ \sigma_{rr} \\ \sigma_{rz} \\ \sigma_{r\theta} \\ \sigma_{\theta z} \end{bmatrix} \tag{2}$$

For the uniform loading considered in the present study, the shear stresses (σ_{rz}, $\sigma_{r\theta}$) may be approximated as zero consistent with the assumption for thin-walled cylinders.

The reduced strain matrix after incorporating the assumptions of negligible shear stresses (σ_{rz} and $\sigma_{r\theta}$), the constitutive relationship in the global coordinate system is given below:

$$\begin{bmatrix} \varepsilon_{\theta\theta} \\ \varepsilon_{zz} \\ \varepsilon_{rr} \\ \gamma_{\theta z} \end{bmatrix} = \begin{bmatrix} S_{11} & S_{12} & S_{13} & S_{16} \\ S_{21} & S_{22} & S_{23} & S_{26} \\ S_{31} & S_{32} & S_{33} & S_{36} \\ S_{61} & S_{62} & S_{63} & S_{66} \end{bmatrix} \begin{bmatrix} \sigma_{\theta\theta} \\ \sigma_{zz} \\ \sigma_{rr} \\ \sigma_{\theta z} \end{bmatrix} \tag{3}$$

In thermomechanical loading, the total strain $\{\varepsilon\}$ is the superposition of the free-thermal strain $\{\varepsilon^T\}$ and the mechanical strain $\{\varepsilon^\sigma\}$. The strain superposition equation becomes:

$$\{\varepsilon\} = \{\varepsilon^\sigma\} + \{\varepsilon^T\}$$

$$\{\varepsilon\} = [S]\{\sigma\} + \{\varepsilon^T\}$$

The thermoelastic constitutive equation after rearranging, can be written as

$$\begin{bmatrix} \varepsilon_{\theta\theta} \\ \varepsilon_{zz} \\ \varepsilon_{rr} \\ \gamma_{\theta z} \end{bmatrix} = \begin{bmatrix} \overline{S_{11}} & \overline{S_{12}} & \overline{S_{13}} & \overline{S_{16}} \\ \overline{S_{21}} & \overline{S_{22}} & \overline{S_{23}} & \overline{S_{26}} \\ \overline{S_{31}} & \overline{S_{32}} & \overline{S_{33}} & \overline{S_{36}} \\ \overline{S_{61}} & \overline{S_{62}} & \overline{S_{63}} & \overline{S_{66}} \end{bmatrix} \begin{bmatrix} \sigma_{\theta\theta} \\ \sigma_{zz} \\ \sigma_{rr} = 0 \\ \tau_{\theta z} \end{bmatrix} + \begin{bmatrix} \alpha_\theta \\ \alpha_z \\ 0 \\ \alpha_{\theta z} \end{bmatrix} \Delta T \tag{3a}$$

$$\alpha_\theta = m^2\alpha_1 + n^2\alpha_2$$

$$\alpha_z = n^2\alpha_1 + m^2\alpha_2$$

$$\alpha_{\theta z} = 2mn(\alpha_1 - \alpha_2)$$

where $m = \cos(\theta_o)$ and $n = \sin(\theta_o)$

The transformed compliance coefficients (S_{ij}) are expressed in terms of the material properties and the fibre orientation angle, θ_o.

$$S_{11} = \frac{1}{E_{11}} m^4 + \left(\frac{1}{G_{12}} - \frac{2\nu_{12}}{E_{11}} \right) m^2 n^2 + \frac{1}{E_{22}} n^4 \quad (4)$$

$$S_{22} = \frac{1}{E_{11}} n^4 + \left(\frac{1}{G_{12}} - \frac{2?_{12}}{E_{11}} \right) m^2 n^2 + \frac{1}{E_{22}} m^4 \quad (5)$$

$$S_{33} = \frac{1}{E_{33}} \quad (6)$$

$$S_{12} = S_{21} = \left(\frac{1}{E_{11}} + \frac{1}{E_{22}} + \frac{2\nu_{12}}{E_{11}} - \frac{1}{G_{12}} \right) m^2 n^2 - \frac{\nu_{12}}{E_{11}} \quad (7)$$

$$S_{23} = S_{32} = -\frac{\nu_{23}}{E_{22}} m^2 - \frac{\nu_{31}}{E_{33}} n^2 \quad (8)$$

$$S_{13} = S_{31} = -\frac{\nu_{23}}{E_{22}} n^2 - \frac{\nu_{31}}{E_{33}} m^2 \quad (9)$$

$$S_{66} = \left(\frac{4}{E_{11}} + \frac{4}{E_{22}} + \frac{8\nu_{12}}{E_{11}} - \frac{4}{G_{12}} \right) m^2 n^2 + \frac{1}{G_{12}} \quad (10)$$

$$S_{61} = S_{16} = \left(\frac{2}{E_{11}} m^2 - \frac{2}{E_{22}} n^2 - \left(\frac{1}{G_{12}} - \frac{2\nu_{12}}{E_{11}} \right) \left(m^2 - n^2 \right) \right) mn \quad (11)$$

$$S_{62} = S_{26} = \left(\frac{2}{E_{11}} n^2 - \frac{2}{E_{22}} m^2 + \left(\frac{1}{G_{12}} - \frac{2\nu_{12}}{E_{11}} \right) \left(m^2 - n^2 \right) \right) mn \quad (12)$$

$$S_{63} = S_{36} = \left(\frac{-2\nu_{31}}{E_{33}} + \frac{2\nu_{23}}{E_{22}} \right) mn \quad (13)$$

where $m = \cos(q_o)$ and $n = \sin(q_o)$

3. STRESSES

When the thin-walled cylinder subjected to the three types of loading, viz., uniform internal pressure (p), longitudinal load (P) and pure torque (T) about the Z-axis of the cylinder, the resulting stresses are:

$$\sigma_{\theta\theta} = \frac{pR}{t} \quad (14)$$

$$\sigma_{zz} = \frac{P}{2\pi Rt} + \frac{pR}{2t} \quad (15)$$

$$\sigma_{\theta z} = \frac{T}{2\pi R^2 t} \quad (16)$$

where R is the mean radius of the cylindrical shell and t is the thickness of the shell. The radial stress (σ_{rr}) is negligible because of the thin wall assumption.

4. STRAIN-DISPLACEMENT RELATIONS

The strain-displacement equations can be simplified considering that the displacements are independent of θ.

$$\varepsilon_{rr} = \frac{\partial u_r}{\partial r} \qquad \varepsilon_{\theta\theta} = \frac{u_r}{r}$$

$$\varepsilon_{zz} = \frac{\partial u_z}{\partial z} \qquad \gamma_{\theta z} = \frac{\partial u_\theta}{\partial z} \quad (17)$$

where u_r, u_θ and u_z are respectively the displacements in r,θ and z directions. From the above equations, it can be shown that the radial, circumferential and longitudinal displacements can be expressed in terms of strains, the mean radius (R) and z coordinate.

$$u_r = R\varepsilon_{\theta\theta} \quad (18)$$

$$u_\theta = (1 + \varepsilon_{zz}) z\gamma_{\theta z} \quad (19)$$

$$u_z = z\varepsilon_{zz} \quad (20)$$

The angle of rotation ϕ for a cross-section of the cylinder at the coordinate z is given by

$$\Phi = \left(\frac{z}{R}\right)(1+\varepsilon_{zz})\gamma_{\theta z} \tag{21}$$

4.1 Unconstrained Effects of Loading

The properties chosen for the analysis of a titanium-matrix composite cylinder with 0.36 volume fraction of SCS6 fibres[13] are taken as

E_{11} = 221 GPa

E_{22} = E_{33} = 145 GPa

G_{12} = G_{13} = 53.2 GPa

G_{23} = 51.7 GPa (22)

ν_{12} = ν_{13} = 0.27

ν_{23} = 0.4

α_1 = 6.15×10^{-6}/°C

α_2 = 7.9×10^{-6}/°C

In the first phase of the analysis, the cylinder is subjected to one loading at a time and its effect on the homogeneous strains ($\gamma_{\theta z}$, ε_{zz}, $\varepsilon_{\theta\theta}$) have been investigated, when the tube is without end constraints and subjected to temperature changes.

The nondimensional parameters corresponding to each loading are expressed as

(a) Effect on $\gamma_{\theta z}$ if only internal pressure (p) alone is acting in addition to temperature change (ΔT^*)

$$C_1 = E_{11}\left[S_{61} + \frac{S_{62}}{2}\right] + G_1\alpha_{\theta z} \tag{23}$$

where $C_1 = \dfrac{E_{11}t}{pR}\gamma_{\theta z}$ is the shear strain parameter due to internal pressure (p) and

$G_1 = \left[\dfrac{\Delta T^* t E_{11}}{pR}\right]$ is the temperature coefficient due to internal pressure (p) and $\alpha_{\theta z} = 2mn(\alpha_1 - \alpha_2)$.

(b) Effect on $\gamma_{\theta z}$ if only axial load P is acting in addition to temperature change (ΔT^*)

$$C_2 = \left(\frac{E_{11}S_{62}}{2\pi}\right) + G_2\alpha_{\theta z} \tag{24}$$

where $C_2 = \left[\dfrac{E_{11}\gamma_{\theta Z}tR}{P}\right]$ is the shear strain due to longitudinal load (P) and $G_2 = \left[\dfrac{\Delta T^* tRE_{11}}{P}\right]$ is the temperature coefficient due to longitudinal load.

(c) Effect on $\gamma_{\theta Z}$ if torque (T) is acting in addition to temperature change (ΔT^*)

$$C_3 = \frac{E_{11}S_{66}}{2\pi} + G_3\alpha_{\theta Z} \tag{25}$$

where $C_3 = \left[\dfrac{E_{11}R^2t\gamma_{\theta Z}}{T}\right]$ is the shear strain parameter due to torque (T) and $G_3 = \left[\dfrac{\Delta T^* R^2 t}{T}\right]$ is the temperature coefficient due to torque (T).

(d) Effect on $\varepsilon_{\theta\theta}$ due to internal pressure (p) in addition to temperature change (ΔT^*)

$$C_4 = E_{11}\left(S_{11} + \frac{S_{12}}{2}\right) + G_1\alpha_\theta \tag{26}$$

where $C_{44} = \left(\dfrac{\varepsilon_{\theta\theta}E_{11}t}{pR}\right)$ is the circumferential strain parameter due to internal pressure (p) and

$\alpha_\theta = m^2\alpha_1 + n^2\alpha_2$

(e) Effect on $\varepsilon_{\theta\theta}$ due to axial load (P) in addition to temperature change (ΔT^*)

$$C_5 = \left(\frac{E_{11}S_{12}}{2\pi}\right) + G_2\alpha_\theta \qquad (27)$$

where $C_5 = \left[\frac{\varepsilon_{\theta\theta} tR}{P}\right]$ is the circumferential strain parameter due to longitudinal load (P).

(f) Effect on $\varepsilon_{\theta\theta}$ due to torque (T) in addition to temperature change (ΔT^*)

$$C_6 = \left(\frac{E_{11}S_{16}}{2\pi}\right) + G_3\alpha_\theta \qquad (28)$$

where $C_6 = \left[\frac{E_{11}tR^2\varepsilon_{\theta\theta}}{T}\right]$ is the circumferential strain parameter due to torque T.

(g) Effect on ε_{zz} due to internal pressure (p) in addition to temperature change ΔT^*

$$C_7 = E_{11}\left(S_{21} + \frac{S_{22}}{2}\right) + G_1\alpha_z \qquad (29)$$

where $C_7 = \left(\frac{E_{11}tR\varepsilon_{zz}}{p}\right)$ is the longitudinal strain parameter due to internal pressure (p) and

$\alpha_Z = n^2\alpha_1 + m^2\alpha_2$

(h) Effect on ε_{zz} due to axial load P in addition to temperature change (ΔT^*)

$$C_8 = \left(\frac{E_{11}S_{22}}{2\pi}\right) + G_2\alpha_z \qquad (30)$$

where $C_8 = \left[\frac{E_{11}Rt}{P}\right]\varepsilon_{zz}$ is the longitudinal strain parameter due to axial load (P).

(i) Effect on ε_{zz} due to torque (T) in addition to temperature change (ΔT^*)

$$C_9 = \left(\frac{E_{11}S_{26}}{2\pi}\right) + G_3\alpha_z \qquad (31)$$

where $C_9 = \left[\frac{E_{11}R^2t}{T}\right]\varepsilon_{zz}$ is the longitudinal strain parameter due to torque (T).

In the second phase of analysis, the effects of constraints have been considered.

(a) Effects of circumferential and end constraints $\varepsilon_{\theta\theta} = 0$ and $\varepsilon_{ZZ} = 0$

$$D_1^* = 2\pi\left[\frac{S_{12}S_{21} - S_{11}S_{22}}{S_{16}S_{22} - S_{12}S_{26}}\right] + 2\pi\left[\frac{\alpha_z S_{12} - \alpha_X S_{22}}{S_{16}S_{22} - S_{12}S_{26}}\right]H_1 \qquad (32)$$

where $D_1^* = \left(\frac{T}{pR^3}\right)$ and $H_1 = \left[\frac{\Delta T^* t}{pR}\right]$

$D_1 = \frac{1}{D_1^*}$ is the pressure-torque parameter and H_1 is the temperature coefficient.

$$D_2 = 2\pi\left[\frac{S_{11} - HS_{21}}{HS_{22} - S_{12}}\right] + 2\pi\left[\frac{H\alpha_z - \alpha_\theta}{HS_{22} - S_{12}}\right]H_1 \qquad (33)$$

where

$$H = \left[\frac{\frac{2}{E_{11}}m^2 - \frac{2}{E_{22}}n^2 - \left(\frac{1}{G_{12}} - \frac{2\nu_{12}}{E_{11}}\right)\left(m^2 - n^2\right)}{\frac{2}{E_{11}}n^2 - \frac{2}{E_{22}}m^2 + \left(\frac{1}{G_{12}} - \frac{2\nu_{12}}{E_{11}}\right)\left(m^2 - n^2\right)}\right]$$

and $D_2 = \left(\frac{P}{pR^2}\right)$ is the longitudinal load – pressure parameter.

(b) Effects of torsional and end-constraints

$\gamma_{\theta Z} = 0$ and $\varepsilon_{ZZ} = 0$

$$D_3 = 2\pi\left[\frac{S_{61}S_{22} - S_{21}S_{62}}{S_{26}S_{62} - S_{66}S_{22}}\right] + 2\pi\left[\frac{\alpha_{\theta z}S_{22} - \alpha_z S_{62}}{S_{16}S_{62} - S_{66}S_{22}}\right]H_1 \qquad (34)$$

where $D_3 = \left(\frac{T}{pR^3}\right)$ is the torque–pressure parameter and

$$D_4 = 2\pi\left[\frac{2S_{26}S_{61} + S_{26}S_{62} - 2S_{66}S_{21} - S_{22}S_{66}}{2\left(S_{22}S_{66} - S_{62}S_{26}\right)}\right] + 2\pi\left[\frac{\alpha_{\theta z}S_{16}S_{62} - \alpha_z S_{66}S_{22}}{S_{22}S_{66} - S_{62}S_{26}}\right]H_1 \quad (35)$$

where $D_4 = \left(\frac{P}{pR^2}\right)$ is the longitudinal load-pressure parameter.

The nondimensional parameter for the angle of rotation becomes:

$$\varphi_r = \frac{\phi E_{11} t}{pR} = C_1\left(1 + C_4\psi\right) \quad (36)$$

where $\psi = \left(\frac{pR}{E_{11}t}\right)$

The critical situations, which a component is more frequently likely subjected to these conditions, are cylindrical bellows, the high-pressure capacity of fire hoses. The other critical situations include versatile and efficient pressure-controlled actuators that can sustain relatively high strains. Robotics is a logical field of application for such actuators.

5. RESULTS AND DISCUSSION

5.1 Effects of Loading without Constraint

- Effect on $\gamma_{\theta Z}$ (Fig. 2)

The peak value of unrestrained twisting C_1 is occurring at 30° of fibre angle and is observed to be negative which signifies that the tube unwinds due to internal pressure (p).

The max value of twisting C_2 occurs at 60° of the fibre angle when the tube is subjected to axial load P (Fig. 2) and this is a negative value signifying that the tube unwinds due to the application of longitudinal load P. It is also observed that at 30° fibre angle, no twisting occurs due to the compensating effects of shear modulus on axial modulus.

The peak value of unrestrained twisting C_3 occurs when the tube is subjected to twisting at the fibre angle of zero and 90°. The twisting is positive indicating that the tube winds due to the application of twisting moment (Fig.2).

- Effects on circumferential strain, ε_{ZZ} (Fig.3)

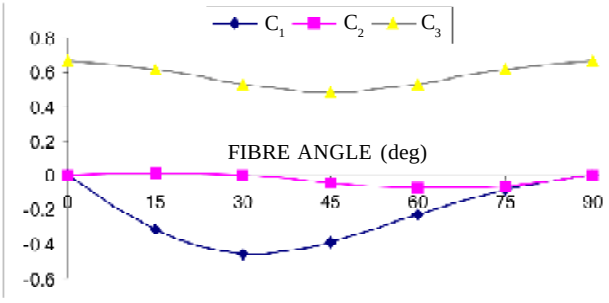

Figure 2. Effect of loading on twisting.

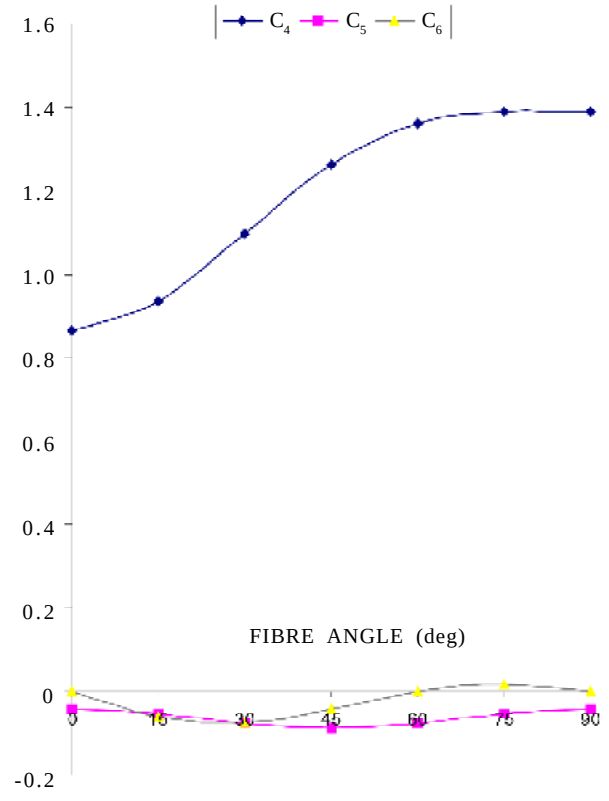

Figure 3. Effect on circumferential strain.

The peak value of C_4 occurs when the fibre angle is 90° due to the effect of internal pressure (p). The peak value of C_5 occurs when the fibre angle is 45° when subjected to the axial load P. The value is negative indicating the contraction of the tube. The peak value of C_6 occurs at the fibre angle 30° due to the application of torque (T) and it is negative indicating contraction.

- Effect on longitudinal strain, ε_{ZZ} (Fig. 4)

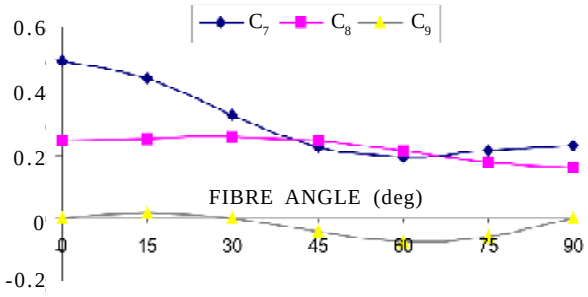

Figure 4. Effect on longitudinal strain.

The peak value of longitudinal strain parameter C_8 occurs when the fibre angle is zero when it is subjected to axial load P. It is justified that when $\theta = 0$, the direction of the applied load is in the perpendicular direction to the maximum stiffness.

The peak value of C_7 occurs at the fibre angle zero when it is subjected to an internal pressure (p) but greater than the effect of longitudinal load P.

The peak value of C_9 occurs at the fibre angle 60°, when it is subjected to a twisting moment, T. The peak value is negative showing that the tube contracts by a maximum amount when the twisting is applied to the tube. It is also observed that there is no effect on longitudinal strain due to the twisting moment when the fibre angle is 30°.

5.2 Effects of Loading with Constraint

- Effects of circumferential and end-constraints:

$$\varepsilon_{\theta\theta} = \varepsilon_{ZZ} = 0$$

The pressure –torque parameter (D_1) is calculated and plotted against the fibre angle which signifies the requirement of internal pressure (p) for a given torque (T) such that the cylinder is fully constrained, ie, $\varepsilon_{ZZ} = \varepsilon_{\theta\theta} = 0$. Maximum value of D_1 occurs at fibre angle 30° (Fig.5). The pressure-longitudinal load parameter (D_2) is calculated and plotted to compute the required pressure for a given value of longitudinal load for full cylinder confinement (Fig. 6).

- Effects of torsional and end-constraints

$$\gamma_{\theta Z} = \varepsilon_{ZZ} = 0$$

The study has been carried out to find the effects of restraining the cylinder from rotation as well as the longitudinal displacement. The torque-pressure parameter (D_3) is plotted against fibre angle (Fig.7) indicating the torque required for a given internal pressure when the cylinder is restrained from rotation and longitudinal displacement. Peak value of D_3 occurs at fibre angle of 30°. The longitudinal load-pressure parameter (D_4) is plotted against the fibre angle, signifying the requirement of longitudinal load for a given internal pressure, when the cylinder is prevented from rotation as well as longitudinal displacement. Peak value of D_4 occurs at fibre angle zero (Fig.8).

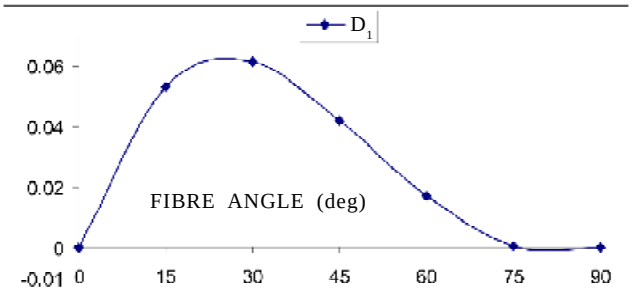

Figure 5. Effect on circumferential and end constraints (pressure-torque parameter).

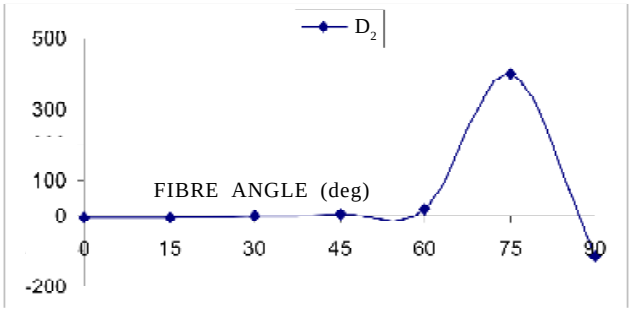

Figure 6. Effect on circumferential and end constraints (pressure-longitudinal load parameter).

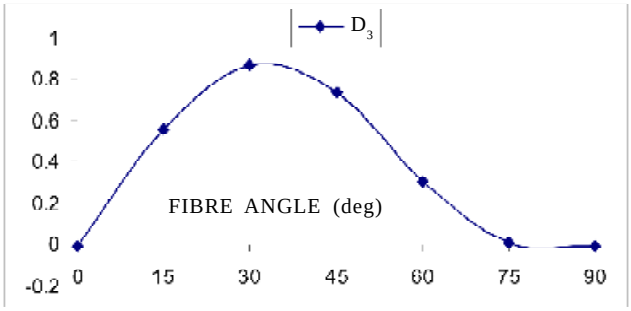

Figure 7. Effect of torsional and end constraints (torque-pressure parameter).

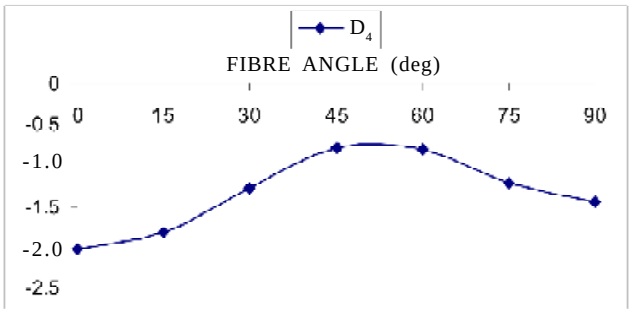

Figure 8. Effect on torsional and end constraints (longitudinal load-pressure parameter).

5.3 Effects of Thermal Loading

In the first phase of analysis unconstrained effects of loading are considered in addition to temperature changes, in the second phase of analysis the effects of constraints (effects of circumferential torsional, and-end constraints) have been considered along with the temperature changes.

5.3.1 Effects of Loading in Addition to Temperature Changes, without Constraint

- Effect on $\gamma_{\theta z}$ (Fig. 9)

The peak value of unrestrained twisting C_1, C_2, C_3 are occurring at the fibre angle 45° and is observed to be negative which signifies that the tube unwinds. Because of thermal loading the tube is unwinding when the tube is subjected to twisting, otherwise the twisting is positive[9] without thermal loads..

- Effects on circumferential strain, $\varepsilon_{\theta\theta}$ (Fig.10)

The peak value of C_4 C_5, C_6 occurs when the fibre angle is 90° due to the effect of internal

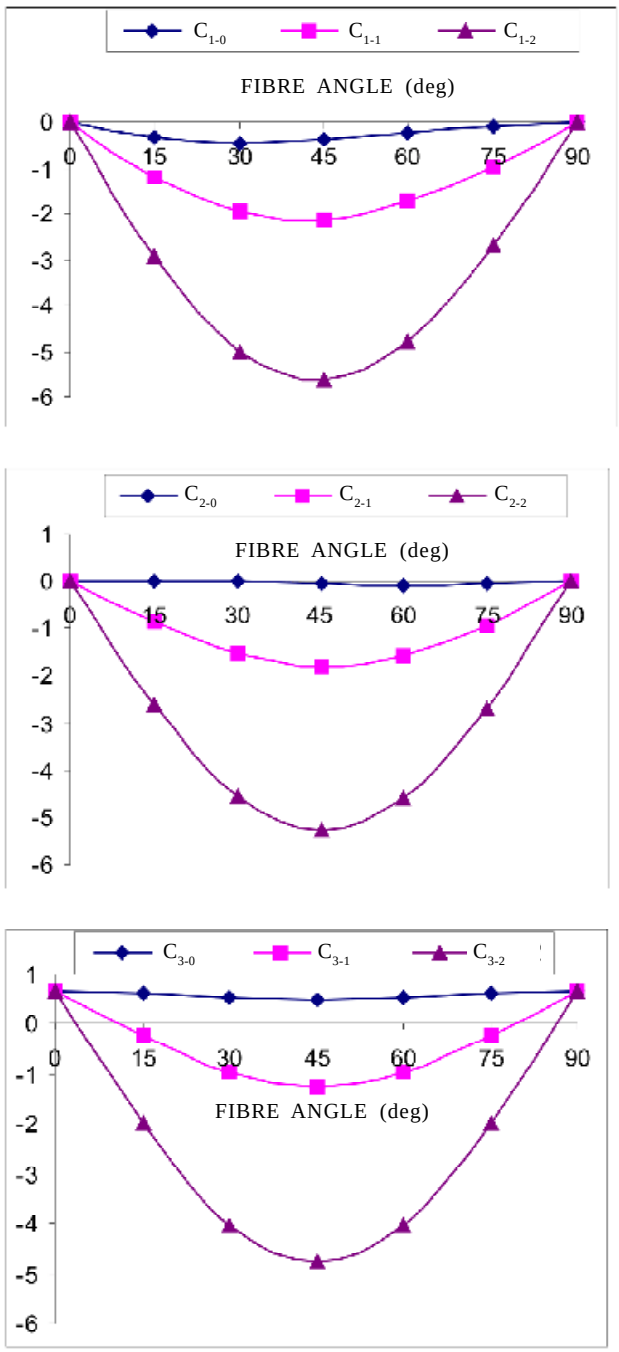

Figure 9. Effect of loading on twisting (with temperature).

pressure (p), axial load (P) and due to the application of torque (T), respectively and all are positive indicating expansion. When thermal loads are not present, C_5, C_6 are negative indicating contraction.

- Effect on longitudinal strain, ε_{zz} (Fig.11)

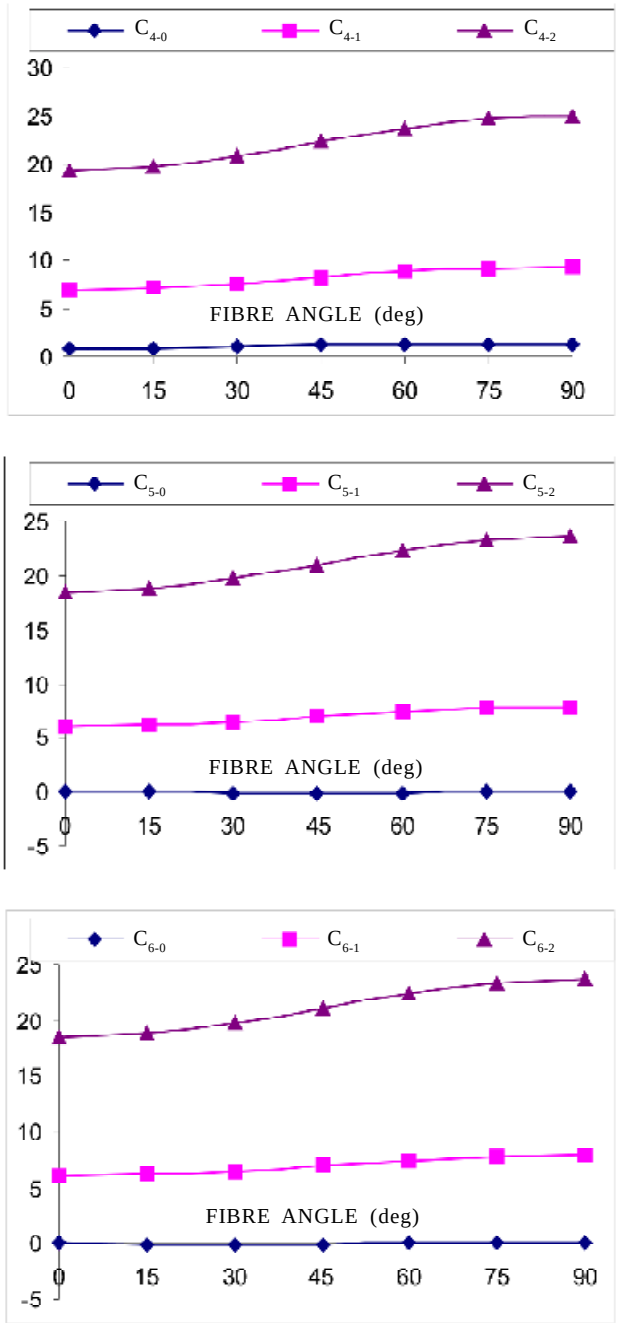

Figure 10. Effect of loading on circumferential strain (with temperature).

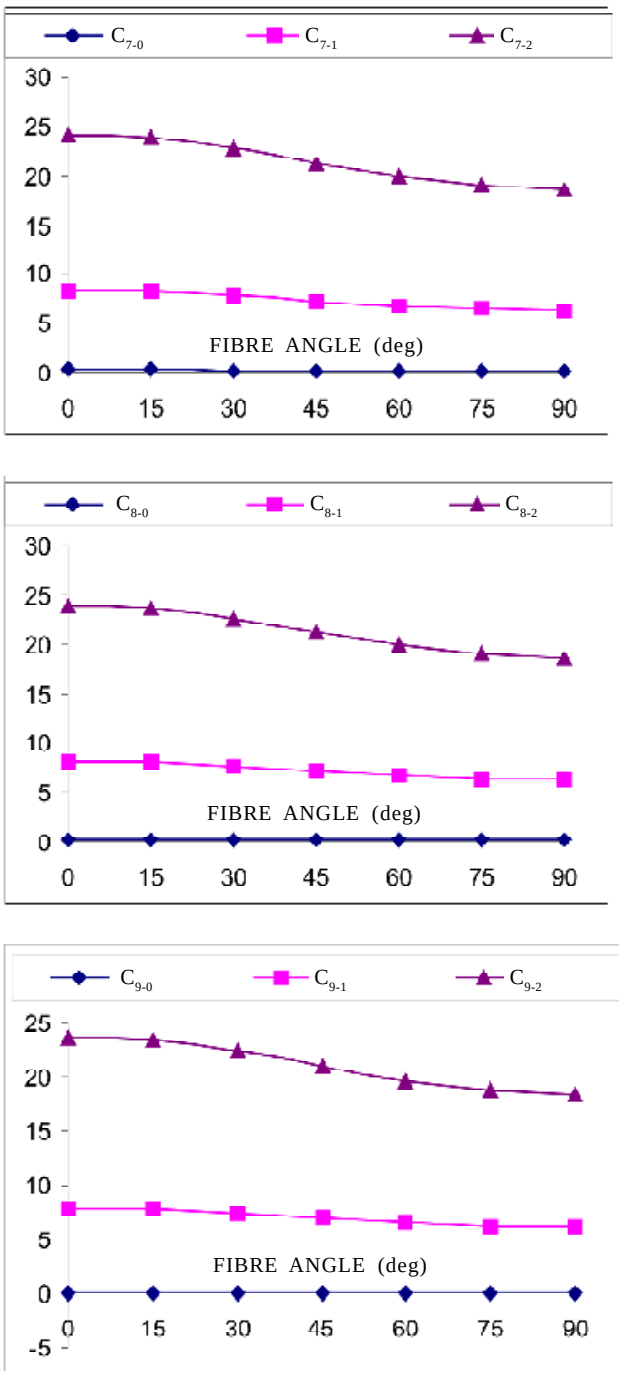

Figure 11. Effect on longitudinal strain (with temperature).

The peak value of longitudinal strain parameter C_7, C_8, C_9 occurs at the fibre angle zero when it is subjected to internal pressure (p), axial load (P) and due to the twisting moment, respectively. It is justified that when $\theta = 0$, the direction of the applied load is in the perpendicular direction to the maximum stiffness.

The peak value of C_9 occurs at the fibre angle is 60° when it is subjected to a twisting moment (T) alone without temperature changes. The peak value is negative showing that the tube contracts by a maximum amount when the twisting is applied to the tube.

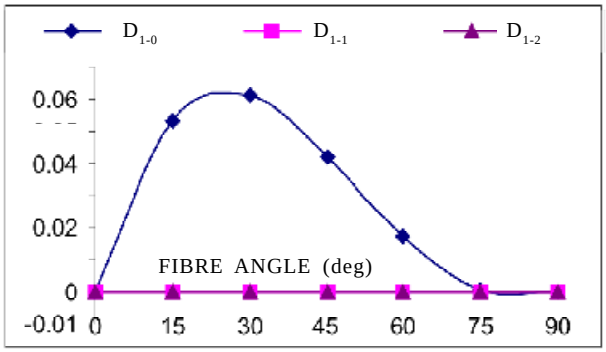

(a)

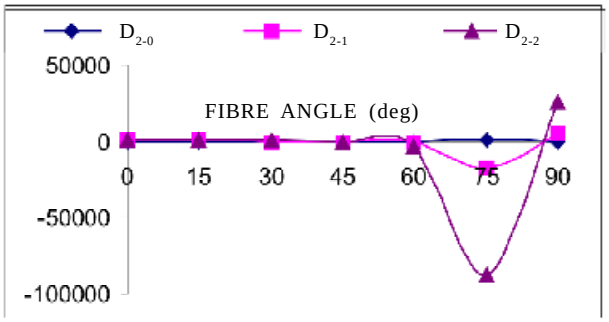

(b)

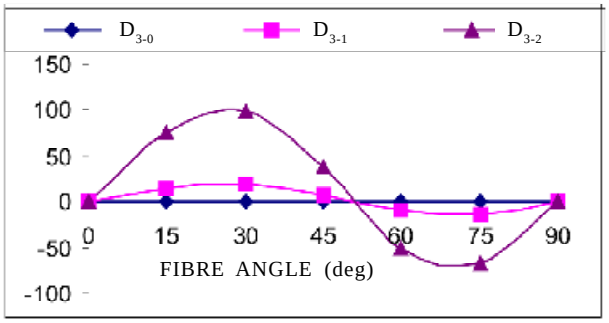

(c)

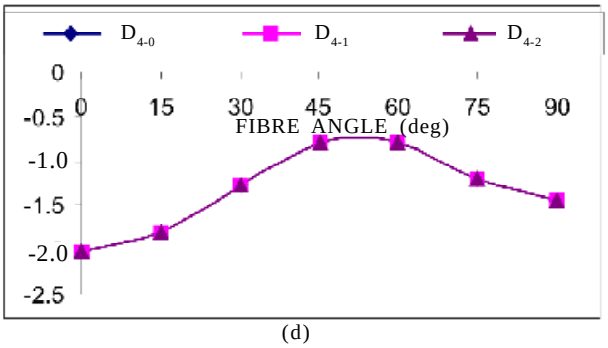

(d)

Figure 12. Effect on circumferential and end constraints : (a) pressure-torque parameter, (b) pressure-longitudinal load parameter, effect of torsional and end constraints, (c) torque-pressure parameter, and (d) logitudinal load-pressure parameter.

5.3.2 Effects of Loading in Addition to Temperature Changes, with Constraint

- Effects of circumferential and end-constrains ($\varepsilon_{\theta\theta} = \varepsilon_{ZZ} = 0$)

The pressure–torque parameter (D_1) is calculated and plotted against the fibre angle, which implies when thermal loads are acting, the pressure torque parameter is zero [Fig.12(a)]. The pressure-longitudinal load parameter (D_2) is calculated and plotted to compute the required pressure for a given value of longitudinal load for full cylinder confinement. It is seen clearly that it is negative with thermal loads [Fig.12(b)].

- Effects of torsional and end-constraints ($\gamma_{\theta Z} = \varepsilon_{ZZ} = 0$)

The study has been carried out to find the effects of restraining the cylinder from rotation as well as the longitudinal displacement . The torque-pressure parameter (D_3) is plotted against fibre angle [Fig.12(c)] indicating the torque required for a given internal pressure when the cylinder is restrained from rotation and longitudinal displacement. Peak value of D_3 occurs at fibre angle, θ_0=30° degrees, but fibre angle nearly 50° onwards it is negative. The longitudinal load-pressure parameter (D_4) is plotted against the fibre angle signifying the requirement of longitudinal load for a given internal pressure when the cylinder is prevented from rotation as well as longitudinal displacement. Peak value of (D_4) occurs at the fibre angle, θ_0= 0 [Fig.12(d)], and the temperature is not having any effect on D_4.

The following tables give peak values of dimensionless parameters and corresponding fibre orientation for different load conditions. From the dimensionless parameters strains and maximum loads can be found.

CONCLUSIONS

From the analysis presented in this paper, the inferences can be summarised as follows:

- It has been observed that maximum twisting occurs when the fibre angle, θ_o = 30° for

Table 1. Effect of loading without constraint

Loading conditions	Dimensionless parameter (max value)		Corresponding fibre orientation (deg)	
	Without thermal loading	With thermal loading	Without thermal loading	With thermal loading
Torsional (twisting) strain parameters (C_1, C_2, C_3 *associated with* $\gamma_{\theta z}$)				
C_1 – Due to the effect of internal pressure (p)	- 0.50	- 5.5	30	45
C_2 – Longitudinal load (P)	- 0.05	- 5.5	60	45
C_3 - Torque (T)	0.70	- 5.5	90	45
Circumferential strain parameters (C_4, C_5, C_6 *associated with* $\varepsilon_{\theta\theta}$)				
C_4 – Due to the effect of internal pressure (p)	1.40	22	90	90
C_5 – Longitudinal load (P)	- 0.05	22	45	90
C_6 - Torque (T)	- 0.025	22	30	90
Longitudinal strain parameters (C_7, C_8, C_9 *associated with* ε_{zz})				
C_7 – Subjected to internal pressure (p)	0.50	24	0	0
C_8 – Axial load (P)	0.25	24	0	0
C_9 - Torque (T)	- 0.05	24	60	0

Table 2. Effect of loading with constraint

Loading conditions	Dimensionless parameter (max value)		Corresponding fibre orientation (deg)	
	Without thermal loading	With thermal loading	Without thermal loading	With thermal loading
Effects of circumferential and end-constraints ($\varepsilon_{\theta\theta} = \varepsilon_{ZZ} = 0$)				
Pressure-torque parameter (D_1)	0.06	0	30	-
Pressure-longitudinal load parameter (D_2)	400	- 80	75	75
Effects of torsional and end-constraints ($\gamma_{\theta z} = \varepsilon_{ZZ} = 0$)				
Torque-pressure parameter (D_3)	0.8	100	30	30
Longitudinal load-pressure parameter (D_4)	- 2.0	- 2.0	0	0

internal pressure (p), but for an axial load (P), this occurs at the fibre angle, $\theta_o = 60°$. For a pure torque T, the maximum twisting deformations occurs when $\theta_o = 90°$.

- The application of internal pressure (p) and axial load (P) effects twisting about the longitudinal axis. The application of T produces a change in cylinder length which is specific to the cylinder made up of orthotropic composite material.

- The maximum longitudinal strain (ε_{zz}) for p occurs at $\theta_o = 0$, and also for axial load (P). The maximum longitudinal strain occurs at, $\theta_o = 60°$ when pure torque T is applied.

- It has been observed that maximum twisting occurs when the fibre angle (θ_o) = 45° for all the three loads when thermal effects are considered. Whereas it occurs at fibre angle θ_o = 30° for internal pressure (p), but for an axial load (P), this occurs at θ_o = 60°, for a pure torque (*T*), the maximum twisting deformations occurs when θ_o = 90° without thermal loads.

- When temperature effects are considered, the pressure-longitudinal load parameter is negative for circumferential and end constraints. The maximum longitudinal strain ε_{zz} occurs at θ_o = 0, for internal pressure (*p*) and also for axial load (*P*) and pure torque (*T*). And the longitudinal strain increases with temperature.

- The study will be useful in designing the pressure-controlled actuators when they are subjected to different constraints.

REFERENCES

1. Wilkins, D.J. & Love, T.S. Combined compression – torsion buckling tests of laminated composite cylindrical shells. *AIAA J. Aircraft*, 1974, **12**(11), 885-89.

2. Waltz, T. & Vinson, J.R. Interlaminar stresses in laminated cylindrical shells of composite materials. *AIAA J. Aircraft*, 1976, **14**(9) 1213-218.

3. El Naschie, M.S. Initial and post buckling of axially compressed orthotropic cylindrical shells. *AIAA J. Aircraft*, 1976, **14**(10), 1502-504.

4. Fujczak, R.R. Torsional fatigue behaviour of graphite-epoxy cylinders. *In* Proceedings of the 2nd International Conference on Composite Materials (ICCM2), 1978, pp. 635-48.

5. Bootan, M. & Tennyson, R.C. Buckling of imperfect anisotropic circular cylinders under combined loading. *In* Proceedings of AIAA/ASME 19th Structures, Structural Dynamics, Material Conference, 1978, pp. 351-58.

6. Montague, P. Experimental behaviour of double-skinned composite, circular cylindrical shells under external pressure. *J. Mech. Engg. Sci.*, 1978, **20** (1), 21-34.

7. Ynceoglu, V. & Updike, D.P. Stress concentration in bonded multilayer cylindrical shells. ASCE Preprint 80-656, 1980.

8. Reissner, E. & Tsai, W.T. Pure bending, stretching and testing of anisotropic cylindrical shells. *ASME J. Appl. Mech.*, 1974, **41** 168-74.

9. Wilson, J.F. & Orgill, G. Linear analysis of uniformly stressed, orthotropic cylindrical shells. *ASME J. Appl. Mech.*, 1986, **53**, 249-56.

10. Warwick, C.M. & Clyne, T.W. Development of composite coaxial cylinder stress analysis model and its application to *SiC* monofilament analysis systems. *J. Mater. Sci.*, 1991, **26**, 3817-827.

11. Mikata, Y. & Taya, M. Stress field in a coated continuous fibre composite subjected to thermo mechanical loadings. *J. Comp. Mater.*, 1984, **19**(11), 554-78.

12. Rama Murty, G. & Reddy, M.C.S., Analysis of titanium metal-matrix orthotropic cylindrical shell subjected to uniform stress. Indo-German Workshop on High Temperature Fibre Composite Materials, 11-15 September 2000, Dept. of Mech. Engg., Institute of Technology, Banaras Hindu University, Varanasi.

13. Hyer, M.W. Stress analysis of fibre-reinforced composite materials. Mc Graw Hill, 1998.

14. Herakovich, C.T. Mechanics of fibrous composites. John Wiley & Sons, Inc., 1998.